Pnicogen bonds between X=PH3 (X = O, S, NH, CH2) and phosphorus and nitrogen bases

ARTICLE *in* THE JOURNAL OF PHYSICAL CHEMISTRY A · FEBRUARY 2014

Impact Factor: 2.69 · DOI: 10.1021/jp411623h · Source: PubMed

THE JOURNAL OF PHYSICAL CHEMISTRY A

Article

pubs.acs.org/JPCA

Pnicogen Bonds between X═PH_3 (X = O, S, NH, CH_2) and Phosphorus and Nitrogen Bases

Ibon Alkorta,* Goar Sánchez-Sanz, and José Elguero

Instituto de Química Médica (IQM-CSIC), Juan de la Cierva, 328006 Madrid, Spain

Janet E. Del Bene*

Department of Chemistry, Youngstown State University, Youngstown, Ohio 44555, United States

Supporting Information

ABSTRACT: Ab initio MP2/aug′-cc-pVTZ calculations have been carried out to investigate the pnicogen bonded complexes formed between the acids O═PH_3, S═PH_3, HN═PH_3, and H_2C═PH_3 and the bases NH_3, NCH, N_2, PH_3, and PCH. All nitrogen and phosphorus bases form complexes in which the bases are lone pair electron donors. The binding energies of complexes involving the stronger bases NH_3, NCH, and PH_3 differentiate among the acids, but the binding energies of complexes with the weaker bases do not. These complexes are stabilized by charge transfer from the lone pair orbital of N or P to the σ^*P═A orbital of X═PH_3, where A is the atom of X directly bonded to P. PCH also forms complexes with the X═PH_3 acids as a π electron donor to the σ^*P═A orbital. The binding energies and the charge-transfer energies of the π complexes are greater than those of the complexes in which PCH is a lone pair donor. Whether the positive charge on P increases, decreases, or remains the same upon complex formation, the chemical shieldings of ^{31}P decrease in the complexes relative to the corresponding monomers. ^{1p}J(P−N) and ^{1p}J(P−P) values correlate best with the corresponding P−N and P−P distances as a function of the nature of the base. ^1J(P−A) values do not correlate with P−A distances. Rather, the absolute values of ^1J(P−O), ^1J(P−S), and ^1J(P−N) decrease upon complexation. Decreasing ^1J(P−A) values correlate linearly with increasing complex binding energies. In contrast, ^1J(P−C) values increase upon complexation and correlate linearly with increasing binding energies.

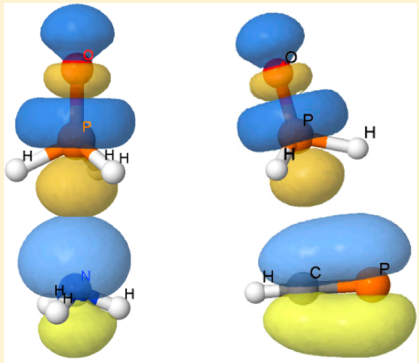

INTRODUCTION

Organophosphonates (OPs) are compounds with the general formula X═PRR′R″ with X = O, S, NH, or CH_2 and R, R′, R″ = H or a variety of other substituents.[1] These compounds are highly toxic, interacting with acetyl cholinesterases (AChEs) in biochemical systems. OPs have been used as nerve gases (chemical warfare agents) and insecticides. Because of their high toxicity and uses, understanding the interaction mechanisms of OPs with AChEs is an issue of immediate practical concern. Selected OPs are illustrated in Figure 1.

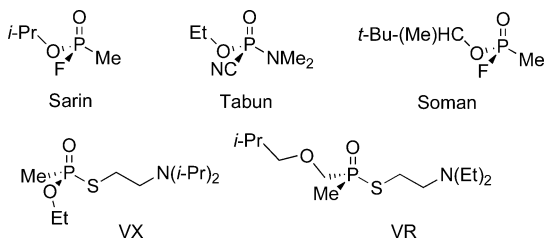

Figure 1. Examples of organophosphonates.

Related to the OPs are the phosphatranes, a class of tricyclic cage-like heterocycles having a transannular dative bond between nitrogen and phosphorus, as illustrated in Figure 2.[2] Although not previously recognized as such, the dative P···N interactions in these systems are pnicogen interactions. The pnicogen bond arises when a pnicogen atom such as N, P, or As acts as an electron accepting Lewis acid to form a molecular complex. In such complexes, it is possible for two pnicogen

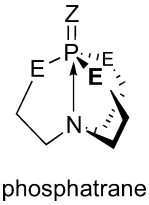

Figure 2. Structure of phosphatrane, illustrating lone pair donation by N to P. Z may be O or S, and E may be O or CH_2.

Received: November 26, 2013
Revised: February 5, 2014
Published: February 18, 2014

dx.doi.org/10.1021/jp411623h | J. Phys. Chem. A 2014, 118, 1527−1537

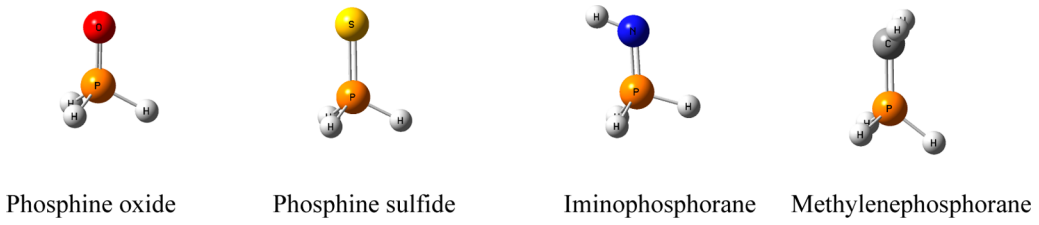

Figure 3. Model Lewis acids $O{=}PH_3$, $S{=}PH_3$, $HN{=}PH_3$, and $H_2C{=}PH_3$.

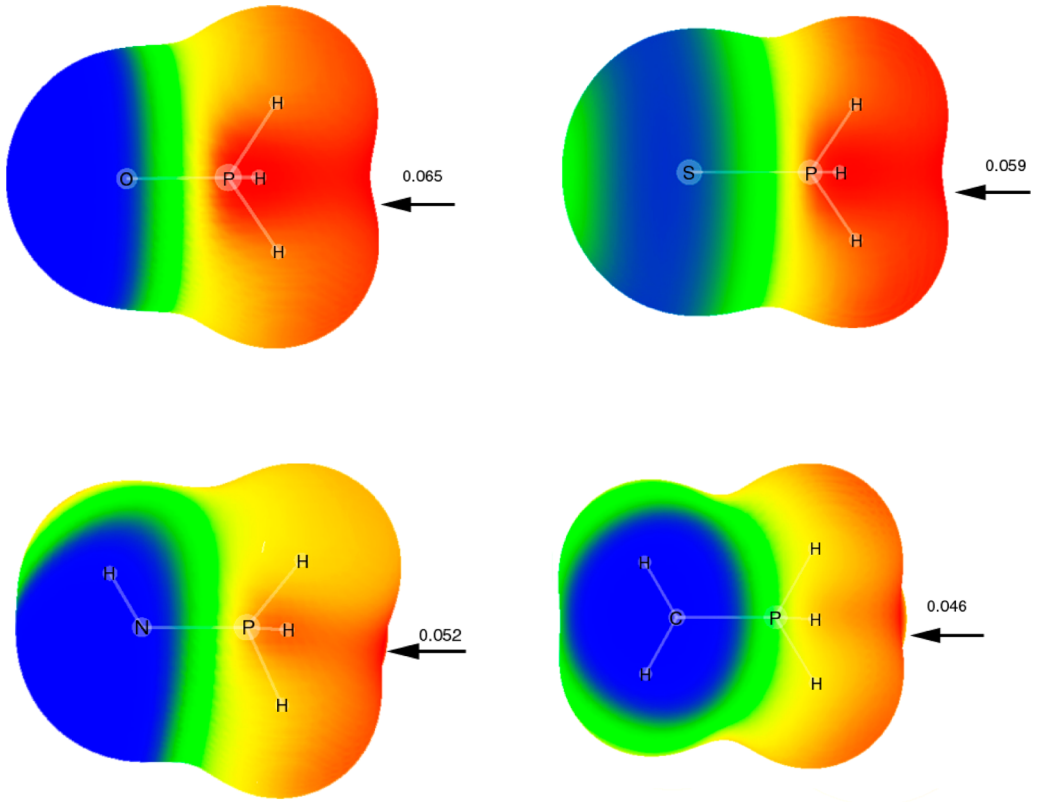

Figure 4. MEPs of $O{=}PH_3$, $S{=}PH_3$, $HN{=}PH_3$, and $H_2C{=}PH_3$. The color coding is red > 0.030 > yellow > 0.0 > green > −0.030 > blue. Values of the MEP maxima (au) are indicated in the figure.

atoms such as P and N to act as both electron pair donors and electron pair acceptors, forming P···P or P···N bonds. Subsequent to the landmark paper by Hey-Hawkins et al.,[3] there has been a resurgence of interest in pnicogen bonds.[4−31] Studies of such bonds have focused on PH_3 and its derivatives. However, in recent papers, we have investigated P···P bonds in two series of complexes, $(H_2C{=}PX)_2$[32] and $H_2C{=}(X)$-$P{:}PXH_2$.[33] In the later series three types of structures were identified. Two of these involve $H_2C{=}(X)P$ and XPH_2 acting as both lone pair donors and electron acceptors through a σ^* orbital. The third structure has $H_2C{=}(X)P$ as a π-electron donor to the $\sigma^*P{-}A$ orbital of PXH_2, with A the atom of X directly bonded to P, and PXH_2 as a lone pair donor to the $\pi^*C{=}P$ orbital of $H_2C{=}PX$. This structure is unique among the pnicogen complexes reported thus far in the literature.

In the present paper we turn our attention to another new type of intermolecular pnicogen bond in complexes with a model of the phosphatrane molecule. As the model we have chosen the phosphorus-containing molecules $X{=}PH_3$, for X = O, S, NH, and CH_2, which are illustrated in Figure 3. These molecules, particularly phosphine oxide, have been the subjects of a large number of theoretical investigations.[34−40] In the present study we examine the pnicogen bonds in complexes in which these molecules interact with the lone pair donating nitrogen bases NH_3, NCH, and N_2 to form P···N bonds, and with PH_3 and PCH to form P···P bonds. Because PCH may also be a π electron donor,[41−43] we have included complexes with this molecule as a π donor as well. In this paper, we report the structures and binding energies of these complexes, their bonding properties, and the NMR properties of ^{31}P chemical shieldings and $^{31}P{-}^{31}P$ spin−spin coupling constants.

METHODS

The structures of the monomers and binary complexes were optimized at second-order Møller−Plesset perturbation theory (MP2)[44−47] with the aug′-cc-pVTZ basis set,[48] which is the Dunning aug-cc-pVTZ basis[49,50] with diffuse functions removed from H atoms. Frequencies were computed to identify equilibrium and transition structures. Only equilibrium structures are reported in this paper. The MP2 calculations were performed using the Gaussian 09 program.[51]

Molecular electrostatic potentials (MEPs) have been calculated and represented on the 0.001 au electron density isosurfaces using the WFA program.[52] This isosurface has been

dx.doi.org/10.1021/jp411623h | J. Phys. Chem. A 2014, 118, 1527−1537

shown to resemble the van der Waals surface.[53] In addition, the natural bond orbital (NBO) method[54] has been used to analyze the stabilizing charge-transfer interactions using the NBO-6 program.[55] Because MP2 orbitals are nonexistent, the charge-transfer energies were evaluated from B3LYP calculations[56,57] with the aug′-cc-pVTZ basis set at the MP2/aug′-cc-pVTZ geometries, so that at least some electron correlation effects would be included. NBO orbitals have been represented with the Jmol program[58] using the tools developed by Marcel Patek.[59]

The absolute shieldings have been calculated at MP2/aug′-cc-pVTZ using the GIAO approximation.[60] Coupling constants were evaluated using the equation-of-motion coupled cluster singles and doubles (EOM-CCSD) method in the CI (configuration interaction)-like approximation[61,62] with all electrons correlated. For these calculations, the Ahlrichs[63] qzp basis set was placed on ^{13}C, ^{15}N, and ^{17}O, and the qz2p basis set on ^{31}P, ^{33}S, and ^{1}H of X═PH_3. The Dunning cc-pVDZ basis set has been placed on other H atoms.[49] All of the Ramsey terms, namely the paramagnetic spin orbit (PSO), diamagnetic spin orbit (DSO), Fermi contact (FC), and spin dipole (SD), have been evaluated. The EOM-CCSD calculations were performed using ACES II[64] on the IBM Cluster 1350 (Glenn) at the Ohio Supercomputer Center.

RESULTS AND DISCUSSION

Monomers. The molecular electrostatic potentials of the X═PH_3 molecules exhibit a region of positive charge on the side opposite the X═P bond, as illustrated in Figure 4. These regions are analogous to those generated by electronegative atoms, have been designated σ−holes,[29] and are suitable for interaction with a Lewis base. The maximum values of the MEPs decrease as expected in the order O > S > NH > CH_2. The MEP minima for the phosphorus and nitrogen bases are reported in Table 1. They indicate a region of negative charge along the principal symmetry axis of each molecule at N for the nitrogen bases and at P of PH_3. However, the MEP of PCH at P along its symmetry axis is positive. This is consistent with the observations that PCH does not protonate at P, and that the proton-bound homodimer $(HCP)_2H^+$ does not form at P but through the π system nearer C.[41,42] However, PCH does form linear hydrogen bonded complexes with itself, FH, and ClH. Although the linear complexes are local minima on their potential surfaces, they are 5, 8, and 12 kJ/mol, respectively, less stable that the corresponding π complexes.

Table 1. MEP Minima (au) for NH_3, NCH, N_2, PH_3, and PCH along the Principal Symmetry Axis of Each Molecule[a]

molecule	minima	molecule	minima
NH_3	−0.0595	PH_3	−0.0257
NCH	−0.0509	PCH	+0.0072
N_2	−0.0136		

[a]The minimum value of the MEP for the π system of PCH is −0.014 au.

Complexes. *Structures and Binding Energies.* The structures and total energies of complexes X═PH_3:NZ and X═PH_3:PZ are given in Table S1 of the Supporting Information. The binding energies and intermolecular distances of these complexes are reported in Table 2. All of the N and P lone pair electron donors, including PCH, form complexes with all X═PH_3 molecules. From Table 2 it can be seen that for a given X═PH_3, the binding energies of the stronger bases decrease in the order NH_3 > NCH > PH_3. The weaker bases N_2 and PCH have binding energies between −6 and −7 kJ/mol with all X═PH_3.

Figure 5 provides a plot of the binding energies of these complexes as a function of the minimum values of the MEPs of the N and P bases, which are identified along the MEP axis. The correlation coefficients R^2 of the trendlines vary from 0.90 for complexes with H_2C═PH_3 to 0.94 for those with O═PH_3. It is interesting to note that the stronger bases NH_3, NCH, and PH_3 have binding energies that differentiate among the acids X═PH_3. However, the binding energies of complexes with the weaker bases N_2 and PCH show little dependence on the nature of the acid. The slopes of the trendlines decrease in the order O═PH_3 > S═PH_3 > HN═PH_3 > H_2C═PH_3, and the trendlines converge at the binding energies of X═PH_3:PCH.

Figure 6 provides a different view of the relationship between the strengths of the acids and bases in a plot of the binding energies of the complexes versus the maximum values of the MEPs for the X═PH_3 molecules, which are identified along the MEP maxima axis. The trendlines indicate that the stronger bases NH_3, NCH, and PH_3 have binding energies that depend on the nature of X═PH_3. This is also true but to a much lesser extent for the weaker base N_2. However, the trendline for PCH is flat, showing that the binding energy is essentially independent of the acid. The trendlines for complexes with the bases NH_3, NCH, PH_3, and N_2 have correlation coefficients R^2 of 0.98 or greater. In contrast, the correlation coefficient for PCH is 0.65.

Table 2. MP2/aug′-cc-pVTZ Interaction Energies (ΔE, kJ/mol) and Intermolecular Distances (R, Å) of Complexes X═PH_3:NZ and X═PH_3:PZ

	ΔE			R(P···N)		
	NH_3	NCH	N_2	NH_3	NCH	N_2
O═PH_3	−20.42	−17.75	−7.15	3.145	3.120	3.287
S═PH_3	−18.87	−17.27	−6.86	3.241	3.190	3.362
HN═PH_3	−16.23	−14.30	−6.26	3.249	3.201	3.357
H_2C═PH_3	−13.93	−12.58	−5.71	3.331	3.266	3.416
	ΔE		R(P···P)			
	PH_3	PCH	PH_3	PCH		
O═PH_3	−12.61	−6.60	3.629	3.684		
S═PH_3	−11.73	−6.83	3.732	3.729		
HN═PH_3	−10.52	−6.38	3.713	3.690		
H_2C═PH_3	−9.32	−6.16	3.767	3.752		

dx.doi.org/10.1021/jp411623h | J. Phys. Chem. A 2014, 118, 1527−1537

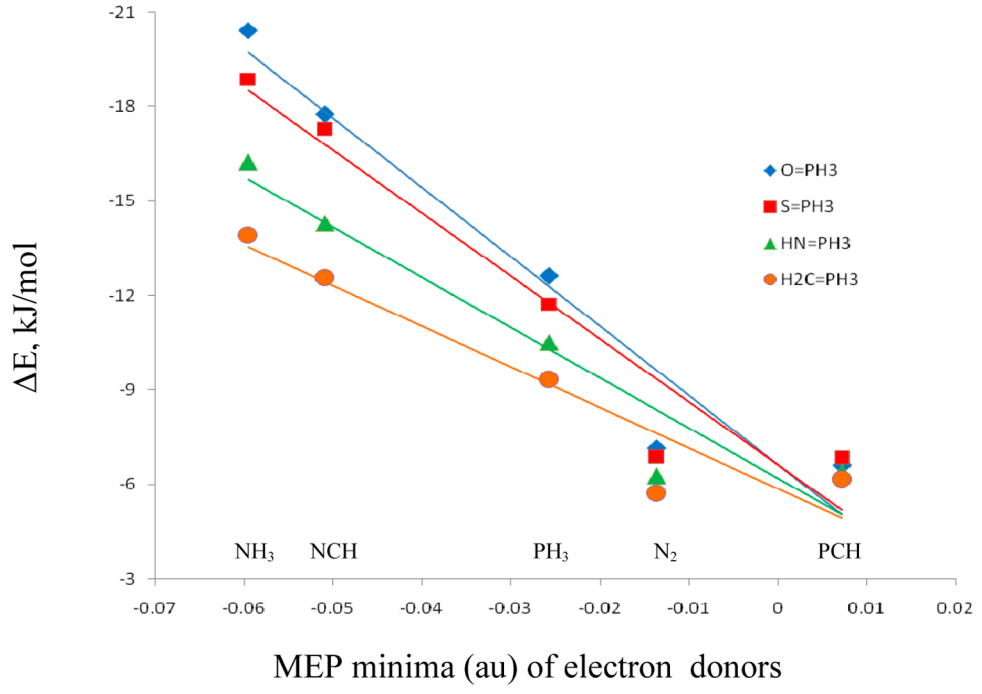

Figure 5. Binding energies of complexes of X═PH_3 with P and N bases as a function of the MEP minima of the bases. Each vertical stack of points is identified by the corresponding base.

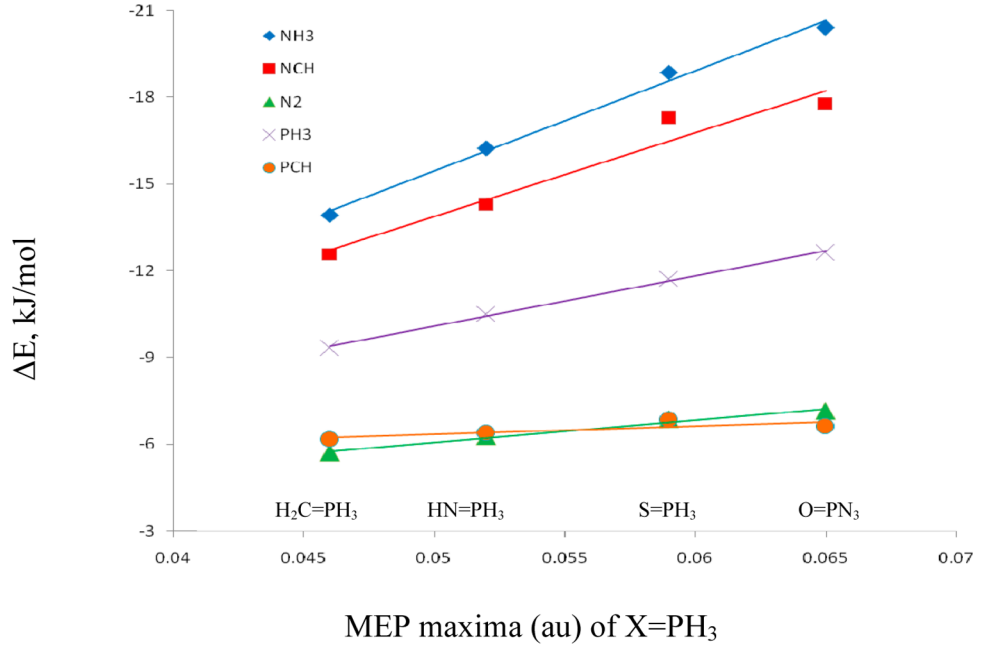

Figure 6. Binding energies of complexes of X═PH_3 with P and N bases as a function of the MEP maxima of the acids. Each vertical stack of points is identified by the corresponding X═PH_3 molecule.

We have also examined the potential surfaces of X═PH_3:PCH for complexes in which the interaction involves the π system of PCH. The structures and energies of these complexes are reported in Table S2 of the Supporting Information. Consistent with the interaction of PCH with other acids, the π complexes X═PH_3:PCH are more stable than the corresponding lone pair complexes, with binding energies of −11.68, −11.56, −9.97, and −11.24 kJ/mol with O═PH_3, S═PH_3, HN═PH_3, and H_2C═PH_3, respectively. Although the binding energies are greater, the P−P distances in these complexes are longer, ranging from 3.81 to 3.93 Å. The P−P−C angles vary between 65 and 69°, allowing for a closer approach of the C atom of PCH to P of X═PH_3, since the C≡P π bond is polarized toward C.

NBO Analyses. Many well-known noncovalent interactions, such as hydrogen bonding and halogen bonding, are stabilized by charge transfer from an occupied orbital of the electron donor to a low-lying virtual orbital of the electron acceptor.[65,66] Table 3 reports the stabilizing charge-transfer energies for the pnicogen-bonded complexes X═PH_3:NZ and X═PH_3:PZ.

dx.doi.org/10.1021/jp411623h | J. Phys. Chem. A 2014, 118, 1527−1537

Table 3. Stabilizing Charge-Transfer Energies (kJ/mol) from the Lone Pair of P or N to the σ^* P═A orbital of X═PH_3[a]

acid/base	NH_3	NCH	N_2	PH_3	PCH
O═PH_3	9.7	6.2	3.7	6.7	3.4
S═PH_3	7.7	5.1	2.8	4.5	2.6
HN═PH_3	7.8	5.1	3.2	5.4	3.5
H_2C═PH_3	6.2	4.2	2.6	4.1	2.7

[a]A is the atom of X directly bonded to P.

Charge transfer occurs from the lone pair of P or N to the antibonding σ^*P═A orbital, where A is the atom of X bonded directly to P. Figure 7a illustrates the lone-pair orbital of NH_3 interacting with the σ^*P═O orbital of O═PH_3. The charge-transfer energies for these complexes are within ±3.2 kJ/mol of the charge-transfer energy of 6.5 kJ/mol for the N lone pair to the σ^*P−H orbital in the complex H_3P:NH_3. For comparison, the N lone pair orbital and the σ^*P−H orbital for this complex are shown in Figure 7b. In X═PH_3 complexes with the nitrogen bases, charge-transfer energies are largest when O═PH_3 is the acid, and smallest when H_2C═PH_3 is the acid. The energies for S═PH_3 and HN═PH_3 complexes are intermediate and similar. For the phosphorus base PH_3, the charge-transfer energies are largest with O═PH_3 and HN═PH_3 as the acids, and smaller and similar for the remaining two acids. When PCH is the base, charge-transfer energies are larger and similar with O═PH_3 and HN═PH_3, and smaller and similar with S═PH_3 and H_2C═PH_3. With respect to the bases, NH_3 always has the largest charge-transfer energy, and PCH and N_2 have similar, relatively small charge-transfer energies.

To what extent are the binding energies of these complexes related to the charge-transfer energies? Figure 8 presents a plot of the binding energies versus the charge-transfer energies as a function of the nature of the base. From this plot it can be seen that the binding energies of the complexes tend to increase as the charge-transfer energies increase, although there is some scatter in the data. The correlation coefficient R^2 for a linear relationship is 0.809.

The figures in Table S1 of the Supporting Information indicate that a bond path can connect the N or P of a base to the P of X═PH_3. However, in some cases bond paths connect from the base N or P atoms to the P and the H atoms of the acid, or just to the H atoms or the P−H bonds. Does this indicate that there are no pnicogen bonds in these complexes? That is very unlikely, given that the charge-transfer energies are always from the N or P lone pairs to the σ^*P═A orbitals of X═PH_3, and are comparable to the charge-transfer energy for the pnicogen bonded H_3P:NH_3 complex. Moreover, the charge-transfer energies from the N or P lone pair to the σ^*P−H orbitals of X═PH_3 are negligibly small. The orbital representation of charge transfer for the complex HN═PH_3:NH_3 which has a bond path involving H atoms is illustrated in Figure 7c. The bond path connections to H atoms seen in Table S1 of the Supporting Information may simply be a consequence of the diffuseness of the σ^*P═A orbital of X═PH_3, and should not be interpreted as an indication of the absence of a pnicogen bond.

The bond paths for X═PH_3:PCH π complexes are illustrated in Table S2 of the Supporting Information. Although the bond paths suggest that the bonds involve the π orbital interacting with the H atoms of X═PH_3, the orbital interaction representations clearly illustrate that the interactions involve the π orbital of PCH and the σ^*P═A orbital, as illustrated in Figure 7d for O═PH_3:PCH. Indeed, the πP═C → σ^*P═A charge-transfer energies are greater than the P(lp) → σ^*P═A energies for the corresponding X═PH_3:PCH lone-pair complexes, indicating that the π complexes are also stabilized by pnicogen bonds.

^{31}P Chemical Shieldings. Although the charge on P may increase, remain the same, or decrease upon complexation, the ^{31}P absolute chemical shieldings always decrease in X═PH_3:NZ and X═PH_3:PZ complexes relative to the corresponding monomers. These decreases range from −8 to −27 ppm, as can be seen from the data of Table 4. Thus, there is no correlation between the change in the charges on P atoms and the change in the ^{31}P chemical shieldings.

For a given X═PH_3 molecule, the decrease in the ^{31}P absolute chemical shieldings follows the same order as the decrease in the binding energies of the nitrogen bases (NH_3 > NCH > N_2). Similarly, for a given X═PH_3, the shieldings decrease in the same order as the corresponding binding energies for the phosphorus bases (PH_3 > PCH). Correlations between decreasing chemical shieldings and decreasing binding energies were observed previously in complexes of PO_2F and PO_2Cl with nitrogen bases.[67]

Spin−Spin Coupling Constants. ^{1p}J(P−N) and ^{1p}J(P−P). Total spin−spin coupling constants ^{1p}J(P−N) and ^{1p}J(P−P) and their components are reported in Table S3 of the

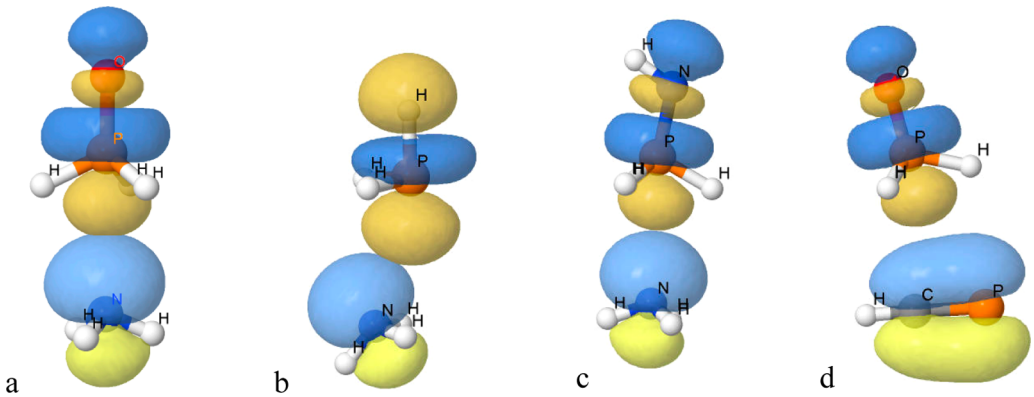

Figure 7. Depiction of the orbitals involved in charge-transfer interactions in complexes. NH_3 lone pair with the (a) σ^*P═O orbital of O═PH_3, (b) σ^*P−H orbital of H_3P, (c) σ^*P═N orbital of HN═PH_3. (d) πP═C orbital of PCH with the σ^*P═O orbital of O═PH_3. Charge-transfer energies are 9.7, 6.5, 7.8, and 4.5 kJ/mol, respectively.

dx.doi.org/10.1021/jp411623h | J. Phys. Chem. A 2014, 118, 1527−1537

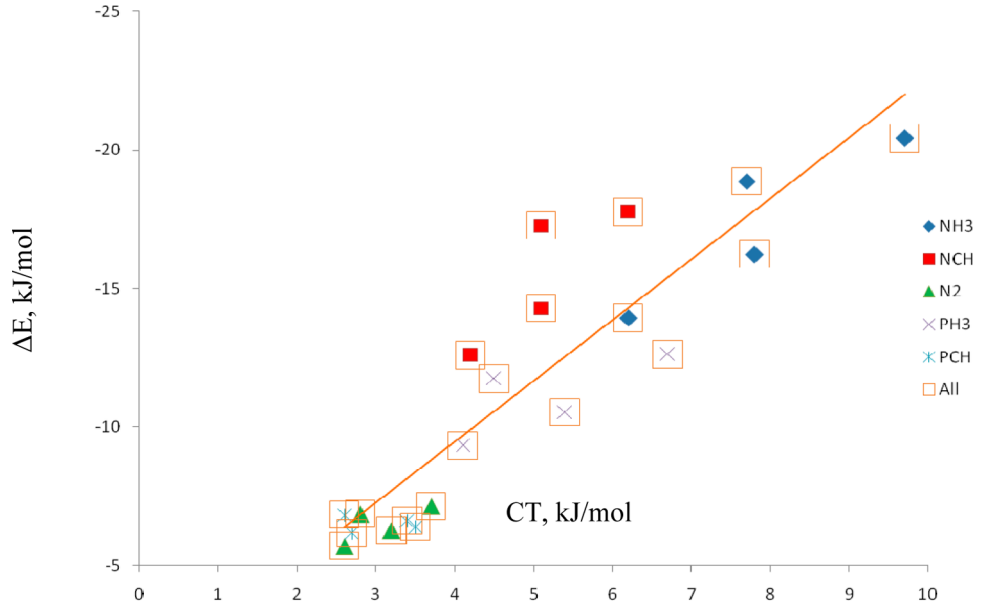

Figure 8. Binding energies of complexes X═PH_3:Base versus the charge-transfer energies of the complexes as a function of the nature of the base.

Table 4. ^{31}P Absolute Chemical Shieldings for X═PH_3 Monomers and Changes in Shieldings upon Complex Formation

	O═PH_3:Base	S═PH_3:Base	HN═PH_3:Base	H_2C═PH_3:Base
monomers	426.0	451.2	450.0	473.0
X═PH_3:Base				
Base = NH_3	−20.3	−26.8	−23.9	−24.2
Base = NCH	−17.3	−22.1	−20.2	−19.8
Base = N_2	−9.1	−12.0	−10.6	−11.1
Base = PH_3	−18.8	−24.7	−22.1	−22.3
Base = PCH	−8.2	−12.5	−11.9	−13.1

Table 5. Intermolecular Distances (R, Å) and ^{1p}J(P−N) and ^{1p}J(P−P) Spin−Spin Coupling Constants (Hz) for Complexes of X═PH_3 with Nitrogen and Phosphorus Bases

	R(P−N)	^{1p}J(P−N)		R(P−P)	^{1p}J(P−P)
O═PH_3:Base					
Base = NH_3	3.145	−19.9	Base = PH_3	3.629	150.8
Base = NCH	3.120	−17.7	Base = PCH	3.684	92.3
Base = N_2	3.287	−8.7			
S═PH_3:Base					
Base = NH_3	3.241	−14.1	Base = PH_3	3.732	105.9
Base = NCH	3.190	−12.5	Base = PCH	3.729	68.1
Base = N_2	3.362	−5.5			
HN═PH_3:Base					
Base = NH_3	3.249	−13.9	Base = PH_3	3.713	107.2
Base = NCH	3.201	−12.6	Base = PCH	3.690	75.4
Base = N_2	3.357	−6.0			
H_2C═PH_3:Base					
Base = NH_3	3.331	−9.6	Base = PH_3	3.767	75.5
Base = NCH	3.266	−8.9	Base = PCH	3.752	53.7
Base = N_2	3.416	−4.1			

Supporting Information. These data illustrate the dominance of the FC term on ^{1p}J(P−N) and ^{1p}J(P−P). The individual PSO, DSO, and SD terms have absolute values no greater than 0.4 Hz, and the FC term differs from total J by 0.5 Hz or less. Thus, the FC term is demonstrated once again to be an excellent approximation to ^{1p}J for coupling across a pnicogen bond.

The total coupling constants ^{1p}J(P−N) and ^{1p}J(P−P) and the corresponding P−N and P−P distances are reported in Table 5. All ^{1p}J(P−N) are negative and all ^{1p}J(P−P) are positive. Because the magnetogyric ratio of ^{15}N is negative and that of ^{31}P is positive, the reduced coupling constants ^{1p}K(P−N) and ^{1p}K(P−P) are both positive. Of course the intermolecular P−N and P−P distances are significantly different, a reflection of the difference between the atomic radii of N and P. For a given acid, the intermolecular distances increase in the order NCH < NH_3 < N_2, but the coupling

dx.doi.org/10.1021/jp411623h | J. Phys. Chem. A 2014, 118, 1527−1537

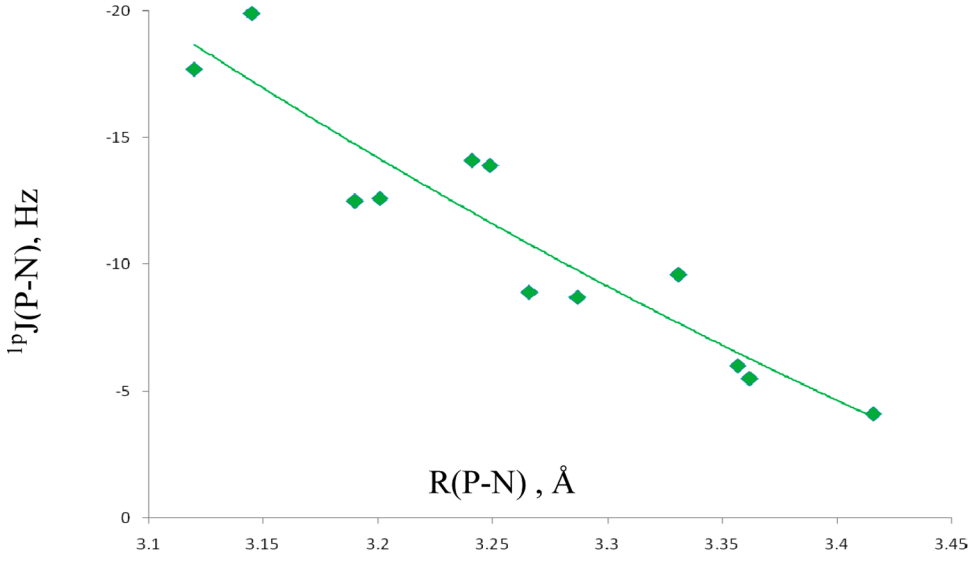

Figure 9. ^{1p}J(P−N) versus the P−N distance for complexes with P···N bonds.

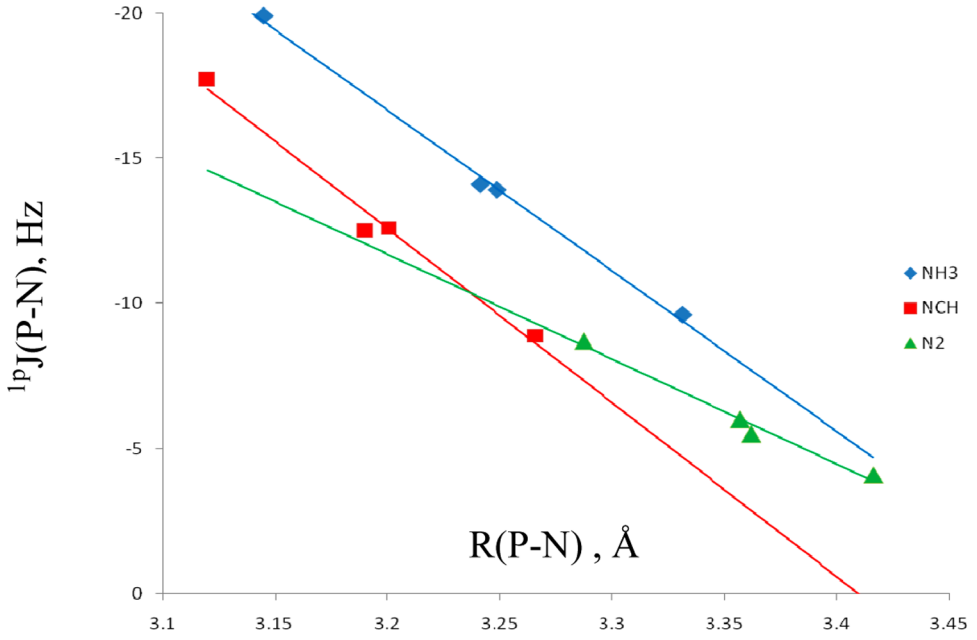

Figure 10. ^{1p}J(P−N) versus the P−N distance as a function of the nature of the base.

constants decrease in absolute value in the order NH_3 > NCH > N_2. To what extent do these two variables correlate? Figure 9 presents a plot of ^{1p}J(P−N) versus the P−N distance for these complexes. The second-order trendline has a correlation coefficient R^2 of 0.868. What is very interesting in this graph is the appearance of four sets of two data points with similar P−N distances and coupling constants. How do these arise?

Figure 10 provides a plot of ^{1p}J(P−N) versus the P−N distance as a function of the nature of the base. ^{1p}J(P−N) values are well correlated with P−N distances for a given base, as evident from the linear trendlines that have correlation coefficients R^2 between 0.983 and 0.997. From this graph it can be seen that for each base there is one point at a shorter distance, two at similar intermediate distances, and one at a longer distance. Thus, the pairs of points at similar distances correspond to the same base with two different acids, S═PH_3 and HN═PH_3.

Coupling constants ^{1p}J(P−P) do not correlate with the P−P distance as a function of the nature of the acid, but the correlation is improved as a function of the base. Figure 11 shows the variation of ^{1p}J(P−P) with distance for these complexes. The linear trendlines for PH_3 and PCH have correlation coefficients of 0.972 for PH_3 and 0.857 for PCH.

Coupling constants ^{1p}J(P−P) for the X═PH_3:PCH π complexes are also dominated by the FC term, with the PSO term contributing −1.0 to −1.5 Hz to total ^{1p}J(P−P). ^{1p}J(P−P) values are 17.4, 11.8, 12.1, and 11.8 Hz for the π complexes with O═PH_3, S═PH_3, HN═PH_3, and H_2C═PH_3, respectively. These values are significantly reduced relative to those for the complexes in which PCH is a lone pair donor, in which case the range is 54−92 Hz. The reduced values in the π complexes are not surprising, given that ^{1p}J(P−P) values are dominated by the FC term which depends on s electron

dx.doi.org/10.1021/jp411623h | J. Phys. Chem. A 2014, 118, 1527−1537

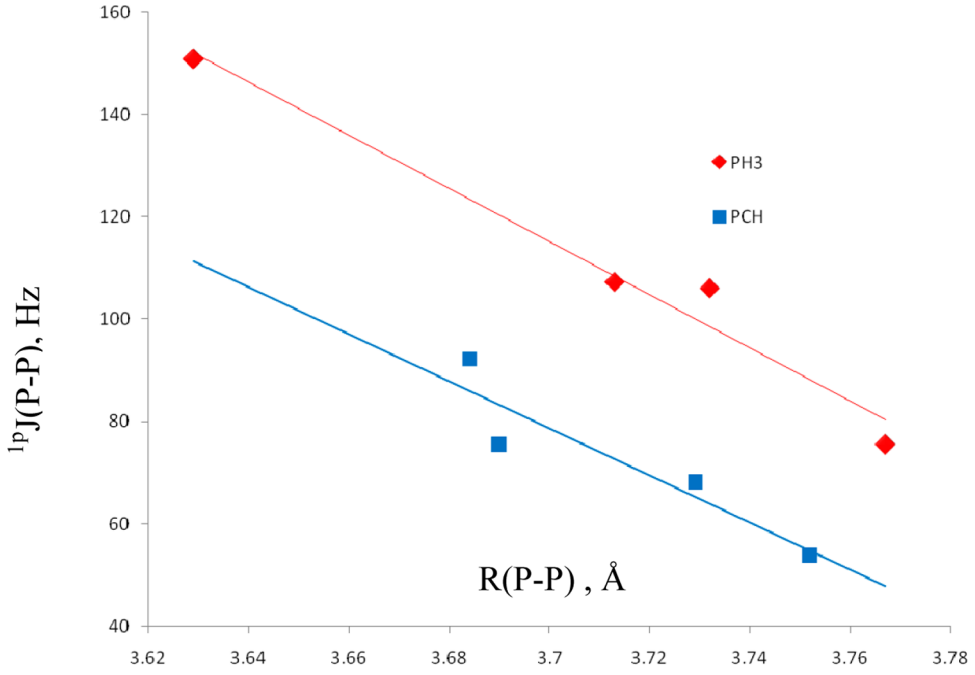

Figure 11. ^{1p}J(P−P) versus the P−P distance, as a function of the base.

Table 6. P−A Distances (R, Å) and ^{1}J(P−A) Spin−Spin Coupling Constants (Hz) for Complexes of X═PH_3 with Nitrogen and Phosphorus Bases[a]

	R(P−O)	^{1p}J(P−O)		R(P−O)	^{1p}J(P−O)
O═PH_3:Base	1.494	198.9			
Base = NH_3	1.497	183.2	Base = PH_3	1.495	190.9
Base = NCH	1.497	185.7	Base = PCH	1.494	196.9
Base = N_2	1.494	193.8			
	R(P−S)	^{1p}J(P−S)		R(P−S)	^{1p}J(P−S)
S═PH_3:Base	1.941	−153.9			
Base = NH_3	1.946	−141.4	Base = PH_3	1.943	−147.6
Base = NCH	1.946	−143.2	Base = PCH	1.940	−152.1
Base = N_2	1.941	−149.9			
	R(P−N)	^{1p}J(P−N)		R(P−N)	^{1p}J(P−N)
HN═PH_3:Base	1.574	72.2			
Base = NH_3	1.577	63.2	Base = PH_3	1.574	66.9
Base = NCH	1.576	64.3	Base = PCH	1.573	70.3
Base = N_2	1.573	68.2			
	R(P−C)	^{1p}J(P−C)		R(P−C)	^{1p}J(P−C)
H_2C═PH_3:Base	1.678	57.7			
Base = NH_3	1.680	67.0	Base = PH_3	1.678	65.3
Base = NCH	1.680	67.2	Base = PCH	1.677	63.0
Base = N_2	1.677	64.7			

[a]A is the atom of X directly bonded to P.

densities, and P−P distances are also longer. ^{1p}J(P−P) values in these complexes do not correlate with the P−P distances.

^{1}J(P−A). Table S4 of the Supporting Information provides the values of ^{1}J(P−A) and its components for complexes X═PH_3:NZ and X═PH_3:PZ, with A the atom of X directly bonded to P. There are three patterns that can be observed from these data. First, all of the one-bond coupling constants are dominated by the FC terms. Second, total J is determined by the FC plus the PSO terms, since the latter are not negligible. However, in all complexes the values of the PSO terms are within ±0.5 Hz of the monomer values. For complexes with the acids O═PH_3, S═PH_3, and HN═PH_3, the PSO terms have the same sign as the corresponding FC terms, but for H_2C═PH_3, the FC and PSO terms are of opposite signs. The third pattern is the sign of the reduced coupling constants ^{1}K(P−A). Because the magnetogyric ratios of C, S, and P are positive and N and O are negative, ^{1}K(P−O), ^{1}K(P−S), and ^{1}K(P−N) are negative, and thus in violation of the Dirac vector model which states that reduced one-bond coupling constants are positive.[68] Such violations are often found when at least one of the coupled atoms has a lone pair of electrons.[69,70] In contrast, H_2C═PH_3 has no lone pairs on P or C, and ^{1}K(P−C) is positive.

dx.doi.org/10.1021/jp411623h | J. Phys. Chem. A 2014, 118, 1527−1537

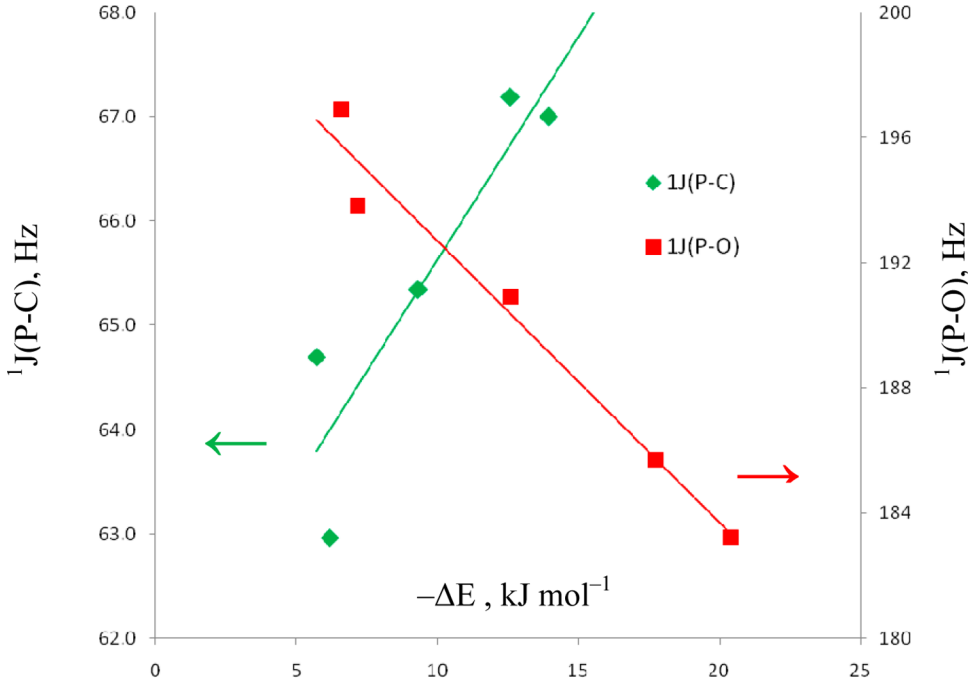

Figure 12. ^1J(P−O) and ^1J(P−C) versus the negative binding energies of complexes with O═PH_3 and H_2C═PH_3 as the acids.

Table 6 reports the P−A distances and ^1J(P−A) coupling constants for complexes of X═PH_3 with the N and P bases. The P−A distances are remarkably insensitive to the presence of P···N or P···P pnicogen bonds, varying from the monomer distances by between −0.001 to +0.005 Å. In contrast, there is a notable variation in ^1J(P−A) upon complex formation. For complexes with O═PH_3, S═PH_3, and HN═PH_3, ^1J(P−A) decreases in absolute value upon complex formation; for complexes with H_2C═PH_3, ^1J(P−C) increases. Since ^1J(P−A) does not reflect changes in the P−A distance, is there another variable with which it correlates?

Figure 12 presents a plot of ^1J(P−O) versus the binding energies of the complexes containing O═PH_3 as the acid. This plot indicates that as the binding energy increases, ^1J(P−O) decreases. The linear trendline has a correlation coefficient R^2 of 0.971. The two points that deviate most from the trendline have the largest ^1J(P−O) values and belong to the two most weakly bound complexes O═PH_3:N_2 and O═PH_3:PCH. These values are closest to the O═PH_3 monomer value. Plots of ^1J(P−S) and ^1J(P−N) are similar to that for ^1J(P−O) and have linear trendlines with correlation coefficients of 0.967 and 0.927, respectively. Figure 12 also provides a plot of ^1J(P−C) versus the binding energies of the complexes with H_2C═PH_3. In contrast to the complexes with the other acids, ^1J(P−C) increases linearly as the binding energy increases, with a correlation coefficient of 0.822. Thus, the characteristics of ^1J(P−C) for complexes with the weakest acid H_2C═PH_3 are consistently different from those of ^1J(P−A) for the remaining acids.

CONCLUSIONS

Ab initio MP2/aug′-cc-pVTZ calculations have been carried out to investigate the pnicogen bonded complexes formed between the acids O═PH_3, S═PH_3, HN═PH_3, and H_2C═PH_3 with the bases NH_3, NCH, N_2, PH_3, and PCH. The results of these calculations support the following statements.

1. All nitrogen and phosphorus bases form complexes in which the N or P base donates a lone pair of electrons to the σ*P═A orbital of X═PH_3, where A is the atom of X directly bonded to P. For each of the acids, the binding energies of complexes with the nitrogen bases decrease in the order NH_3 > NCH > N_2. For the phosphorus bases, the order of decreasing binding energies is PH_3 > PCH. Although the binding energies of complexes involving the stronger bases NH_3, NCH, and PH_3 differentiate among the acids X═PH_3, the binding energies of complexes with the weaker bases N_2 and PCH do not.

2. Charge transfer from the lone pair of the base to the σ*P═A orbital of the acid stabilizes X═PH_3:NZ and X═PH_3:PZ complexes. Complexes with NH_3 have the largest charge-transfer energies, whereas complexes with the weak bases N_2 and PCH have relatively small and similar charge-transfer energies.

3. PCH also forms pnicogen bonded complexes by acting as a π electron donor to the σ*P═A orbital of X═PH_3. The binding energies and the charge-transfer energies of the resulting complexes are greater than the binding energies and charge-transfer energies of complexes in which PCH is a lone pair donor.

4. Whether the charge on P increases, decreases, or remains the same upon complexation, the ^{31}P chemical shieldings always decrease in the complexes relative to the corresponding monomers. There is no correlation between the changes in the charges on P and the changes in the chemical shieldings.

5. Although EOM-CCSD ^{1p}J(P−N) values correlate with the P−N distance, the correlation is improved when examined as a function of the base. Similarly, ^{1p}J(P−P) values correlate with the P−P distance when examined as a function of the base.

6. The P−A distances are remarkably insensitive to complex formation, but ^1J(P−A) values are not. For the acids O═PH_3, S═PH_3, and HN═PH_3, absolute values of ^{1p}J(P−A) decrease upon complexation, and the decrease correlates linearly with increasing binding energies. In contrast, ^1J(P−C) values for

dx.doi.org/10.1021/jp411623h | J. Phys. Chem. A 2014, 118, 1527−1537

complexes with $H_2C{=}PH_3$ increase upon complexation, and increase linearly as the complex binding energies increase.

■ ASSOCIATED CONTENT

Supporting Information

Geometries, energies, and molecular graphs of complexes $X{=}PH_3$:NZ and $X{=}PH_3$:PZ; components of $^{1p}J(P{-}N)$ and $^{1p}J(P{-}P)$ for these complexes; $^{1}J(P{-}A)$ and its components for monomers and complexes; full refs 51 and 64. This information is available free of charge via the Internet at http://pubs.acs.org.

■ AUTHOR INFORMATION

Corresponding Authors

*I. Alkorta: e-mail, ibon@iqm.csic.es.

*J. E. Del Bene: e-mail, jedelbene@ysu.edu.

Notes

The authors declare no competing financial interest.

■ ACKNOWLEDGMENTS

This work was carried out with financial support from the Ministerio de Economía y Competitividad (Project No. CTQ2012-35513-C02-02) and Comunidad Autónoma de Madrid (Project MADRISOLAR2, ref S2009/PPQ1533). Thanks are also given to the Ohio Supercomputer Center and CTI (CSIC) for their continued support.

■ REFERENCES

(1) Hosea, N. A.; Berman, H. A.; Taylor, P. Specificity and Orientation of Trigonal Carboxyl Esters and Tetrahedral Alkylphosphonyl Esters in Cholinesterases. *Biochemistry* **1995**, *34*, 11528−11536.

(2) Galasso, V. Theoretical Study of the Structure and Bonding in Phosphatrane Molecules. *J. Phys. Chem. A* **2004**, *108*, 4497−4504.

(3) Zahn, S.; Frank, R.; Hey-Hawkins, E.; Kirchner, B. Pnicogen Bonds: A New Molecular Linker? *Chem.—Eur. J.* **2011**, *17*, 6034−6038.

(4) Solimannejad, M.; Gharabaghi, M.; Scheiner, S. SH···N and SH···P Blue-Shifting H-Bonds and N···P Interactions in Complexes Pairing HSN with Amines and Phosphines. *J. Chem. Phys.* **2011**, *134*, 024312 (1−6).

(5) Scheiner, S. A New Noncovalent Force: Comparison of P···N Interaction with Hydrogen and Halogen Bonds. *J. Chem. Phys.* **2011**, *134*, 094315 (1−9).

(6) Scheiner, S. Effects of Substituents upon the P···N Noncovalent Interaction: The Limits of its Strength. *J. Phys. Chem. A* **2011**, *115*, 11202−11209.

(7) Adhikari, U.; Scheiner, S. Substituent Effects on Cl···N, S···N, and P···N Noncovalent Bonds. *J. Phys. Chem. A* **2012**, *116*, 3487−3497.

(8) Adhikari, U.; Scheiner, S. Sensitivity of Pnicogen, Chalcogen, Halogen and H-Bonds to Angular Distortions. *Chem. Phys. Lett.* **2012**, *532*, 31−35.

(9) Scheiner, S. Can Two Trivalent N Atoms Engage in a Direct N···N Noncovalent Interaction? *Chem. Phys. Lett.* **2011**, *514*, 32−35.

(10) Scheiner, S. Effects of Multiple Substitution upon The P···N Noncovalent Interaction. *Chem. Phys.* **2011**, *387*, 79−84.

(11) Scheiner, S. On the Properties of X···N Noncovalent Interactions for First-, Second-, and Third-Row X Atoms. *J. Chem. Phys.* **2011**, *134*, 164313 (1−9).

(12) Adhikari, U.; Scheiner, S. Comparison of P···D (D = P, N) with other Noncovalent Bonds in Molecular Aggregates. *J. Chem. Phys.* **2011**, *135*, 184306 (1−10).

(13) Scheiner, S.; Adhikari, U. Abilities of Different Electron Donors (D) to Engage in a P···D Noncovalent Interaction. *J. Phys. Chem. A* **2011**, *115*, 11101−11110.

(14) Scheiner, S. Weak H-Bonds. Comparisons of CHO to NHO in Proteins and PHN to Direct PN Interactions. *Phys. Chem. Chem. Phys.* **2011**, *13*, 13860−13872.

(15) Del Bene, J. E.; Alkorta, I.; Sánchez-Sanz, G.; Elguero, J. $^{31}P{-}^{31}P$ Spin−Spin Coupling Constants for Pnicogen Homodimers. *Chem. Phys. Lett.* **2011**, *512*, 184−187.

(16) Del Bene, J. E.; Alkorta, I.; Sánchez-Sanz, G.; Elguero, J. Structures, Energies, Bonding, and NMR Properties of Pnicogen Complexes $H_2XP{:}NXH_2$ (X = H, CH_3, NH_2, OH, F, Cl). *J. Phys. Chem. A* **2011**, *115*, 13724−13731.

(17) Adhikari, U.; Scheiner, S. Effects of Carbon Chain Substituents on the P···N Noncovalent Bond. *Chem. Phys. Lett.* **2012**, *536*, 30−33.

(18) Li, Q.-Z.; Li, R.; Liu, X.-F.; Li, W.-Z.; Cheng, J.-B. Pnicogen−Hydride Interaction between FH_2X (X = P and As) and HM (M = ZnH, BeH, MgH, Li, and Na). *J. Phys. Chem. A* **2012**, *116*, 2547−2553.

(19) Li, Q.-Z.; Li, R.; Liu, X.-F.; Li, W.-Z.; Cheng, J.-B. Concerted Interaction between Pnicogen and Halogen Bonds in $XCl{-}FH_2P{-}NH_3$ (X = F, OH, CN, NC, and FCC). *ChemPhysChem* **2012**, *13*, 1205−1212.

(20) Del Bene, J. E.; Alkorta, I.; Sánchez-Sanz, G.; Elguero, J. Structures, Binding Energies, and Spin−Spin Coupling Constants of Geometric Isomers of Pnicogen Homodimers $(PHFX)_2$, X = F, Cl, CN, CH_3, NC. *J. Phys. Chem. A* **2012**, *116*, 3056−3060.

(21) Del Bene, J. E.; Alkorta, I.; Sánchez-Sanz, G.; Elguero, J. Homo- and Heterochiral Dimers $(PHFX)_2$, X = Cl, CN, CH_3, NC: To What Extent Do They Differ? *Chem. Phys. Lett.* **2012**, *538*, 14−18.

(22) Alkorta, I.; Sánchez-Sanz, G.; Elguero, J.; Del Bene, J. E. Influence of Hydrogen Bonds on the P···P Pnicogen Bond. *J. Chem. Theor. Comp.* **2012**, *8*, 2320−2327.

(23) An, X.-L.; Li, R.; Li, Q.-Z.; Liu, X.-F.; Li, W.-Z.; Cheng, J.-B. Substitution, Cooperative, and Solvent Effects on π Pnicogen Bonds in the FH_2P and FH_2As Complexes. *J. Mol. Model.* **2012**, *18*, 4325−4332.

(24) Bauzá, A.; Quiñonero, D.; Deyà, P. M.; Frontera, A. Pnicogen-π Complexes: Theoretical Study and Biological Implications. *Phys. Chem. Chem. Phys.* **2012**, *14*, 14061−14066.

(25) Alkorta, I.; Sánchez−Sanz, G.; Elguero, J.; Del Bene, J. E. Exploring $(NH_2F)_2$, $H_2FP{:}NFH_2$, and $(PH_2F)_2$ Potential Surfaces: Hydrogen Bonds or Pnicogen Bonds? *J. Phys. Chem. A* **2013**, *117*, 183−191.

(26) Sánchez−Sanz, G.; Alkorta, I.; Elguero, J. Intramolecular Pnicogen Interactions in $PHF{-}(CH_2)n{-}PHF$ (n = 2−6) Systems. *ChemPhysChem* **2013**, *14*, 1656−1665.

(27) Del Bene, J. E.; Alkorta, I.; Sánchez-Sanz, G.; Elguero, J. Phosphorus as a Simultaneous Electron-Pair Acceptor in Intermolecular P···N Pnicogen Bonds and Electron-Pair Donor to Lewis Acids. *J. Phys. Chem. A* **2013**, *117*, 3133−3141.

(28) Grabowski, S. J.; Alkorta, I.; Elguero, J. Complexes between Dihydrogen and Amine, Phosphine, and Arsine Derivatives. Hydrogen Bond versus Pnictogen Interaction. *J. Phys. Chem. A* **2013**, *117*, 3243−3251.

(29) Politzer, P.; Murray, J.; Clark, T. Halogen Bonding and Other σ-Hole Interactions: a Perspective. *Phys. Chem. Chem. Phys.* **2013**, *15*, 11178−11189.

(30) Alkorta, I.; Elguero, J.; Del Bene, J. E. Pnicogen-Bonded Cyclic Trimers $(PH_2X)_3$ with X = F, Cl, OH, NC, CN, CH_3, H, and BH_2. *J. Phys. Chem. A* **2013**, *117*, 4981−4987.

(31) Sánchez-Sanz, G.; Trujillo, C.; Solimannejad, M.; Alkorta, I.; Elguero, J. Orthogonal Interactions Between Nitryl Derivatives and Electron Donors: Pnictogen Bonds. *Phys. Chem. Chem. Phys.* **2013**, *15*, 14310−14318.

(32) Del Bene, J. E.; Alkorta, I.; Elguero, J. Characterizing Complexes with Pnicogen Bonds Involving sp^2 Hybridized Phosphorus Atoms: $(H_2C{=}PX)_2$ with X = F, Cl, OH, CN, NC, CCH, H, CH_3, and BH_2. *J. Phys. Chem. A* **2013**, *117*, 6893−6903.

(33) Del Bene, J. E.; Alkorta, I.; Elguero, J. Properties of Complexes $H_2C{=}(X)P{:}PXH_2$, for X = F, Cl, OH, CN, NC, CCH, H, CH3, and BH_2: P···P Pnicogen Bonding at σ-holes and π-holes. *J. Phys. Chem. A.* **2013**, *117*, 11592−11604.

(34) Schmidt, M. W.; Yabushita, S.; Gordon, M. S. Structure, Bonding, and Internal Rotation in Phosphine Oxide (H_3PO), Hydroxyphosphine (H_2POH), and Hydroxyfluorophosphine (HFPOH). *J. Phys. Chem.* **1984**, *88*, 382−389.
(35) Cramer, C. J.; Dykstra, C. E.; Denmark, S. E. An Ab Initio Study of the [1,2] Proton Transfer from Phosphine Oxide to Phosphinic Acid. *Chem. Phys. Lett.* **1987**, *136*, 17−21.
(36) Dobado, J. A.; Martínez-García, H.; Molina Molina, J.; Sundberg, M. R. Chemical Bonding in Hypervalent Molecules Revised. Application of the Atoms in Molecules Theory to Y_3X and Y_3XZ (Y = H or CH_3; X = N, P or As; Z = O or S) Compounds. *J. Am. Chem. Soc.* **1998**, *120*, 8461−8471.
(37) Chesnut, D. B.; Savin, A. The Electron Localization Function (ELF) Description of the PO Bond in Phosphine Oxide. *J. Am. Chem. Soc.* **1999**, *121*, 2335−2336.
(38) Alkorta, I.; Elguero, J. Theoretical Study of Strong Hydrogen Bonds between Neutral Molecules: The Case of Amine Oxides and Phosphine Oxides as Hydrogen Bond Acceptors. *J. Phys. Chem. A* **1999**, *103*, 272−279.
(39) Weselowski, S. S.; Brinkmann, N. R.; Valeev, E. F.; Schaefer, H. F., III; Repasky, M. P.; Jorgensen, W. L. Three-versus Four-Coordinate Phosphorus in the Gas Phase and in Solution: Treacherous Relative Energies for Phosphine Oxide and Phosphinous Acid. *J. Chem. Phys.* **2002**, *116*, 112−122.
(40) Molina, P.; Alajarín, M.; López Leonardo, C.; Claramunt, R. M.; Foces-Foces, M. C.; Cano, F. H.; Catalán, J.; de Paz, J. L. G.; Elguero, J. Experimental and Theoretical Study of the R_3P+-X- Bond. Case of Betaines Derived from N-Iminophosphoranes and Alkyl Isocyanates. *J. Am. Chem. Soc.* **1989**, *111*, 355−363.
(41) Del Bene, J. E.; Alkorta, I.; Elguero, J. The Structure of Protonated HCP: A Classical or non-Classical Ion? *Chem. Phys. Lett.* **2006**, *429*, 23−26.
(42) Alkorta, I.; Elguero, J.; Del Bene, J. E. HCP and H_3C−CP as Proton Acceptors in Protonated Complexes Containing Two Phosphorus Bases:Structures, Binding Energies, and Spin−Spin Coupling Constants. *J. Phys. Chem. A* **2007**, *111*, 9924−9930.
(43) Alkorta, I.; Sanchez-Sanz, G.; Elguero, J.; Del Bene, J. E. FCl:PCX Complexes: Old and New Types of Halogen Bonds. *J. Phys. Chem. A* **2012**, *116*, 2300−2308.
(44) Pople, J. A.; Binkley, J. S.; Seeger, R. Theoretical Models Incorporating Electron Correlation. *Int. J. Quantum Chem., Quantum Chem. Symp.* **1976**, *S10*, 1−19.
(45) Krishnan, R.; Pople, J. A. Approximate Fourth-Order Perturbation Theory of the Electron Correlation Energy. *Int. J. Quantum Chem.* **1978**, *14*, 91−100.
(46) Bartlett, R. J.; Silver, D. M. Many-Body Perturbation Theory Applied to Electron Pair Correlation Energies. I. Closed-Shell First-Row Diatomic Hydrides. *J. Chem. Phys.* **1975**, *62*, 3258−3268.
(47) Bartlett, R. J.; Purvis, G. D. Many-Body Perturbation Theory, Coupled-Pair Many-Electron Theory, and the Importance of Quadruple Excitations for the Correlation Problem. *Int. J. Quantum Chem.* **1978**, *14*, 561−581.
(48) Del Bene, J. E. Proton Affinities of Ammonia, Water, and Hydrogen Fluoride and their Anions: a Quest for the Basis-Set Limit Using the Dunning Augmented Correlation-Consistent Basis Sets. *J. Phys. Chem.* **1993**, *97*, 107−110.
(49) Dunning, T. H., Jr. Gaussian Basis Sets for Use in Correlated Molecular Calculations. I. The Atoms Boron Through Neon and Hydrogen. *J. Chem. Phys.* **1989**, *90*, 1007−1023.
(50) Woon, D. E.; Dunning, T. H., Jr. Gaussian Basis Sets for Use in Correlated Molecular Calculations. V. Core-valence Basis Sets for Boron Through Neon. *J. Chem. Phys.* **1995**, *103*, 4572−4585.
(51) Frisch, M. J.; Trucks, G. W.; Schlegel, H. B.; Scuseria, G. E.; Robb, M. A.; Cheeseman, J. R.; Scalmani, G.; Barone, V.; Mennucci, B.; Petersson, G. A.; et al. *Gaussian 09*; Gaussian, Inc.: Wallingford, CT, 2009.
(52) Bulat, F.; Toro-Labbé, A.; Brinck, T.; Murray, J.; Politzer, P. Quantitative analysis of Molecular Surface Properties. *J. Mol. Model* **2010**, *16*, 1679−1691.
(53) Bader, R. F.W.; Carroll, M. T.; Cheeseman, J. R.; Chang, C. Properties of Atoms in Molecules: Atomic Volumes. *J. Am. Chem. Soc.* **1987**, *109*, 7968−7979.
(54) Reed, A. E.; Curtiss, L. A.; Weinhold, F. Intermolecular Interactions from a Natural Bond Orbital, Donor-Acceptor Viewpoint. *Chem. Rev.* **1988**, *88*, 899−926.
(55) Glendening, E. D.; Badenhoop, J. K.; Reed, A. E.; Carpenter, J. E.; Bohmann, J. A.; Morales, C. M.; Landis, C. R.; Weinhold, F. *NBO 6.0*; University of Wisconsin: Madison, WI, 2013.
(56) Becke, A. D. Density-Functional Thermochemistry. III. The Role of Exact Exchange. *J. Chem. Phys.* **1993**, *98*, 5648−5652.
(57) Lee, C.; Yang, W.; Parr, R. G. Development of the Colle-Salvetti Correlation-Energy Formula into a Functional of the Electron Density. *Phys. Rev. B* **1988**, *37*, 785−789.
(58) Jmol: an Open-Source Java Viewer for Chemical Structures in 3D, version 13.0. http://www.jmol.org/ (accessed on September 26th, 2013).
(59) Patek, M. "Jmol NBO Visualization Helper" program. http://www.marcelpatek.com/nbo/nbo.html (accessed on September 26th, 2013).
(60) Ditchfield, R. Self-consistent Perturbation Theory of Diamagnetism. I. A Gauge-Invariant LCAO (Linear Combination of Atomic Orbitals) Method for NMR Chemical Shifts. *Mol. Phys.* **1974**, *27*, 789−807.
(61) Perera, S. A.; Nooijen, M.; Bartlett, R. J. Electron Correlation Effects on the Theoretical Calculation of Nuclear Magnetic Resonance Spin−Spin Coupling Constants. *J. Chem. Phys.* **1996**, *104*, 3290−3305.
(62) Perera, S. A.; Sekino, H.; Bartlett, R. J. Coupled-Cluster Calculations of Indirect Nuclear Coupling Constants: The Importance of non-Fermi Contact Contributions. *J. Chem. Phys.* **1994**, *101*, 2186−2191.
(63) Schäfer, A.; Horn, H.; Ahlrichs, R. Fully Optimized Contracted Gaussian Basis Sets for Atoms Li to Kr. *J. Chem. Phys.* **1992**, *97*, 2571−2577.
(64) Stanton, J. F.; Gauss, J.; Watts, J. D.; Nooijen, M.; Oliphant, N.; Perera, S. A.; Szalay, P. G.; Lauderdale, W. J.; Gwaltney, S. R.; Beck, S.; et al. ACES II is a program product of the Quantum Theorey Project, University of Florida.
(65) Weinhold, F.; Klein, R. A. What is a Hydrogen Bond? Mutually Consistent Theoretical and Experimental Criteria for Characterizing H-Bonding Interactions. *Mol. Phys.* **2012**, *110*, 565−579.
(66) Grabowski, S. J. Hydrogen and Halogen Bonds are Ruled by the Same Mechanisms. *Phys. Chem. Chem. Phys.* **2013**, *15*, 7249−7259.
(67) Alkorta, I.; Elguero, J.; Del Bene, J. E. Pnicogen Bonded Complexes of PO_2X (X = F, Cl) with Nitrogen Bases. *J. Phys. Chem. A* **2013**, *117*, 10497−10503.
(68) Lynden-Bell, R. M.; Harris, R. K. *Nuclear Magnetic Resonance Spectroscopy*; Appleton Century Crofts: New York, 1969.
(69) Del Bene, J. E.; Elguero, J.; Alkorta, I. Computed Spin−Spin Coupling Constants ^1J(X-Y) in Molecules H_mX−YH_n for X and Y = ^{13}C, ^{15}N, and ^{31}P: Comparisons with Experiment and Insights into the Signs of ^1J(X-Y). *J. Phys. Chem. A* **2004**, *108*, 3662−3667.
(70) Del Bene, J. E.; Elguero, J. Variation of One-bond X−Y Coupling Constants ^1J(X−Y) and the Components of ^1J(X−Y) with Rotation about the X−Y Bond for Molecules H_mX−YH_n, with X, Y = ^{15}N, ^{17}O, ^{31}P, ^{33}S: The Importance of Nonbonding Pairs of Electrons. *J. Phys. Chem. A* **2007**, *111*, 2517−2526.